ELSEVIER

Journal of Organometallic Chemistry 574 (1999) 77–85

Journal of Organometallic Chemistry

Oxidation properties of $Co(\eta^5\text{-}C_5H_5)(C_8H_4S_8)$ and $Co(L)(C_3S_5)$ ($L = \eta^5\text{-}C_5H_5$ and $\eta^5\text{-}C_5Me_5$) and crystal structure of $Co(\eta^5\text{-}C_5Me_5)(C_3S_5)Br$☆

Hiroyuki Mori, Motohiro Nakano, Hatsue Tamura, Gen-etsu Matsubayashi *

Department of Applied Chemistry, Graduate School of Engineering, Osaka University, 1–16 Machikaneyama, Toyonaka, Osaka 560-0043, Japan

Received 18 June 1998

Abstract

$Co(\eta^5\text{-}C_5H_5)(C_8H_4S_8)$ ($C_8H_4S_8^{2-}$ = 2-{(4,5-ethylenedithio)-1,3-dithiole-2-ylidene}-1,3-dithiole-4,5-dithiolate(2−)) was prepared by a reaction of $Co(\eta^5C_5H_5)(CO)I_2$ with $Na_2C_8H_4S_8$ in ethanol. It was oxidized by iodine in benzene and by the ferrocenium cation in dichloromethane to afford $[Co(\eta^5\text{-}C_5H_5)(C_8H_4S_8)]\cdot I_3$ and $[Co(\eta^5\text{-}C_5H_5)(C_8H_4S_8)][PF_6]_{0.7}$, respectively, with the ligand-centered oxidation, which exhibited electrical conductivities of 0.19 and 0.16 S cm^{-1} for compacted pellets at r.t. $Co(\eta^5\text{-}C_5H_5)(C_3S_5)$ and $Co(\eta^5\text{-}C_5Me_5)(C_3S_5)$ ($C_3S_5^{2-}$ = 4,5-disulfanyl-1,3-dithiole-2-thionate(2−)) were oxidized by 0.5 molar amounts of bromine to give one-electron oxidized species, which were disproportionated to the unoxidized and the two-electron oxidized species in solution. The crystal structure of the one-electron oxidized species, $Co(\eta^5\text{-}C_5Me_5)(C_3S_5)Br$, revealed a one-dimensional array of the molecules through sulfur–sulfur non-bonded contacts. This complex exhibits a strong antiferromagnetic interaction in the solid state, but behaves essentially as an insulator.

Keywords: Cyclopentadienyl; Cobalt complex; Dithiolate complex; Crystal structure; Electrical conductivity

1. Introduction

Metal complexes with sulfur-rich dithiolate ligands often become good electrical conductors. Planar $[M(C_3S_5)_2]$-type anion complexes ($C_3S_5^{2-}$ = 4,5-disulfanyl-1,3-dithiole-2-thionate(2−); M = nickel(II), palladium(II), platinum(II) and gold(III)) are known to have high electrical conductivities and some nickel(II) and palladium (II) complexes behave as a superconductor [1–3]. Metal complexes with the $C_8H_4S_8^{2-}$ (2-{(4,5-ethylenedithio)-1,3-dithiole-2-ylidene}-1,3-dithiole-4,5-dithiolate(2−)) [4–6] and $(RS)_2C_6S_6^{2-}$ (2-{4,5-bis(alkylthio)-1,3-dithiole-2-ylidene}-1,3-dithiole-4,5-dithiolate(2−); R = Me and Et) ligands [7,8] as further π-electron delocalized system were also reported to exhibit high conductivities. In these metal complexes, molecular interactions through many sulfur–sulfur non-bonded contacts construct effective electron-conduction pathways in the solid state. Organometallic complexes containing $C_3S_5^{2-}$ and $C_8H_4S_8^{2-}$ ligands are expected to become unique electrical conductors as molecular inorganic–organic composites having columnar and/or layered structures constructed with non-bonded S–S interactions among the sulfur-rich dithiolate ligands. Several C_3S_5–metal complexes containing cyclopentadienyl and pentamethylcyclopentadienyl groups have been studied as electroactive compounds [9–18]. Although they have non-planar geometries, the oxidized species are expected to form new packings in the solid state to become electrical conductors. Thus, oxidation properties of the complexes are of interest.

☆ Dedicated to the memory of the late Professor Rokuro Okawara.

* Corresponding author.

0022-328X/99/$ - see front matter
PII: S0022-328X(98)00926-7

In this work, Co(η^5-C_5H_5)($C_8H_4S_8$) has been prepared. Oxidation properties of this complex and of Co(η^5-C_5H_5)(C_3S_5) and Co(η^5-C_5Me_5)(C_3S_5) and electrical conductivities of the oxidized species of Co(η^5-C_5H_5)($C_8H_4S_8$) have been studied. The crystal structure of Co(η^5-C_5Me_5)(C_3S_5)Br has been clarified by the X-ray structural analysis. A part of this work has appeared as a communication [19].

2. Experimental

2.1. Synthetic studies

All the following reactions were performed under an argon atmosphere. The reagents, 4,5-bis(cyanoethylthio) - 1,3 - dithiole - 2 - [(4,5 - ethylenedithio) - 1,3-dithiole-2-ylidene], $C_8H_4S_8(CH_2CH_2CN)_2$ [6], Co(η^5-C_5H_5)(CO)I_2 [20], Co(η^5-C_5H_5)(C_3S_5), Co(η^5-C_5Me_5)-(C_3S_5) [10] and [Fe(η^5-C_5H_5)$_2$][PF_6] [21], were prepared according to the literature.

2.2. Co(η^5-C_5H_5)($C_8H_4S_8$) (1)

To a THF (20 cm^3) solution of $C_8H_4S_8(CH_2CH_2CN)_2$ (140 mg, 0.30 mmol), a methanol solution containing 25% NMe_4OH (0.4 cm^3, 1.0 mmol) was added at r.t. The orange solids formed were dissolved in ethanol (20 cm^3). An ethanol (40 cm^3) solution of Co($\eta^5C_5H_5$)(CO)I_2 (120 mg, 0.30 mmol) was added to the solution and was stirred for 10 min at r.t. The black solids obtained were washed with water, ethanol and diethyl ether and dried in vacuo (yield: 140 mg). The solids were dissolved in benzene and the solution was chromatographed on a silica column using the same solvent as an eluent to give dark purple solids of **1** (10% yield). Anal. found: C, 31.54; H, 2.29%. $C_{13}H_9CoS_8$ requires C, 32.49; H, 1.89%. ^{1}H-NMR (270 MHz, C_6D_6, r.t.): δ 2.12 (4H, s, CH_2), 4.37 (5H, s, C_5H_5).

Table 1
Crystallographic data for Co(η^5-C_5Me_5)(C_3S_5)Br (**4**)

Formula	$C_{13}H_{15}BrCoS_5$
M	470.40
Crystal system	Orthorhombic
Space group	*Pmna* (No. 62)
a (Å)	8.320(2)
b (Å)	10.524(2)
c (Å	19.886(2)
V (Å^3)	1741.2(4)
Z	4
$D_{calc.}$ (Mg m^{-3})	1.794
Crystal size (mm^3)	0.22 × 0.22 × × 0.07
F(000)	940.0
μ(Mo–K$_\alpha$) (mm^{-1})	3.87
T (°C)	23
Measured 2θ range (°)	5.0–60.0
No. of unique reflections collected	2910
No. of reflections with $I>2\sigma(I)$	1609
R[a]	0.029
R_w[b]	0.031

[a] $R = \Sigma\ ||F_o|-|F_c||/\Sigma\ |F_o|$.

[b] $R_w = \left[\Sigma\ w(|F_o|-|F_c|)^2/\Sigma\ wF_o^2\right]^{1/2}$, $w^{-1} = \sigma^2(F_o)+0.0001F_o^2$.

Table 2
Atomic co-ordinates and equivalent isotropic thermal parameters for **4**

Atom	x	y	z	B_{eq}[a] (Å^2)
Co	0.79229(7)	0.25	0.08852(3)	2.49(1)
Br	1.03647(6)	0.25	0.12612(3)	3.99(1)
S(1)	0.8125(1)	0.09907(8)	0.01352(4)	3.17(2)
S(2)	0.9588(1)	0.11235(8)	−0.12458(4)	3.90(2)
S(3)	1.0761(3)	0.25	−0.24503(8)	5.87(4)
C(1)	0.8850(3)	0.1843(3)	−0.0520(1)	2.71(6)
C(2)	1.0011(6)	0.25	−0.1694(2)	3.7(1)
C(3)	0.6768(4)	0.3183(3)	0.1813(1)	2.94(6)
C(4)	0.5757(4)	0.3595(3)	0.1282(2)	3.25(7)
C(5)	0.5166(6)	0.25	0.0939(3)	3.7(1)
C(6)	0.7596(6)	0.4013(5)	0.2309(2)	4.43(9)
C(7)	0.5315(7)	0.4947(5)	0.1141(3)	5.3(1)
C(8)	0.4063(7)	0.25	0.0336(3)	5.0(2)

[a] $B_{eq} = (8/3)\pi^2\{U_{11}(aa^*)^2+U_{22}(bb^*)^2+2U_{12}aa^*bb^*\cos\gamma + 2U_{13}aa^*cc^*\cos\beta+2U_{23}bb^*cc^*\cos\alpha\}$.

2.3. [Co(η^5-C_5H_5)($C_8H_4S_8$)]I_3 (2)

To a benzene (400 cm^3) solution of **1** (110 mg, 0.23 mmol), a benzene (40 cm^3) solution of iodine (90 mg, 0.35 mmol) was added with stirring. Black microcrystals of **2** were obtained immediately, which were collected by filtration, washed with benzene, ethanol and diethyl ether, and dried in vacuo (30% yield). Anal. found: C, 18.19; H, 1.12%. $C_{13}H_9CoI_3S_8$ requires C, 18.13; H, 1.05%. The presence of the I_3^- ion was confirmed by the Raman spectrum, as described below.

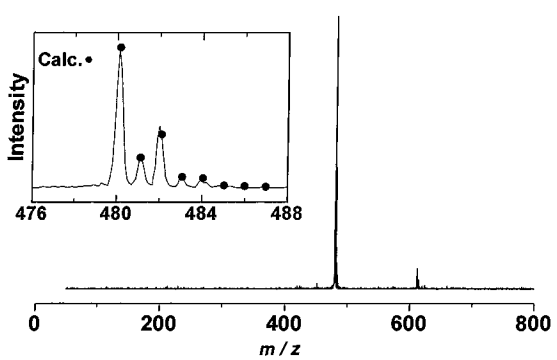

Fig. 1. Positive ion ESI mass spectrum of complex **1** in dichloromethane. In the enlarged spectrum, the calculated intensities (●) based on the isotope distribution of the [Co(η^5-C_5H_5)($C_8H_4S_8$)$_2$]$^+$ cation species are shown.

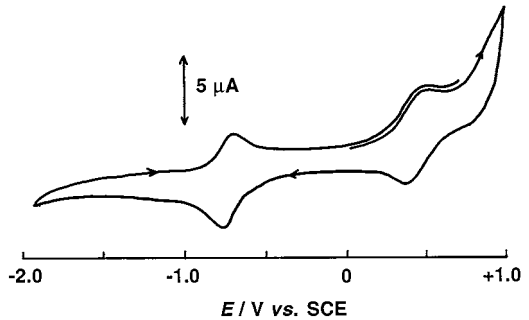

Fig. 2. Cyclic voltammogram of complex **1** (1.0×10^{-4} mol dm^{-3}) in *N*,*N*-dimethylformamide at r.t. Supporting electrolyte: 0.1 mol dm^{-3} [$N^nBu_4ClO_4$]. Sweep rate: 0.1 V s^{-1}.

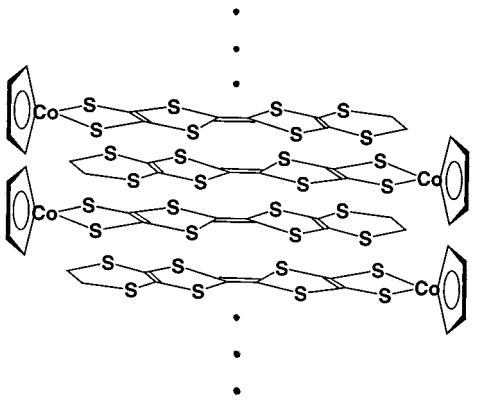

Fig. 4. Assumed molecular array for the oxidized species, complexes **2** and **3**, in the solid state.

2.4. $[Co(\eta^5\text{-}C_5H_5)(C_8H_4S_8)][PF_6]_{0.7}$ (3)

To a dichloromethane (80 cm^3) solution of **1** (50 mg, 0.10 mmol), a dichloromethane (60 cm^3) solution of $[Fe(\eta^5\text{-}C_5H_5)_2][PF_6]$ (33 mg, 0.10 mmol) was added with stirring. Black microcrystals of **3** precipitated immediately, which were collected by centrifugation, washed with dichloromethane and diethyl ether, and dried in vacuo (5% yield). Anal. found: C, 26.91; H, 1.95%. $C_{13}H_9CoF_{4.2}P_{0.7}S_8$ requires C, 26.82; H, 1.56%.

2.5. $Co(\eta\text{-}C_5Me_5)(C_3S_5)Br$ (4)

To a dichloromethane (15 cm^3) solution of $Co(\eta^5\text{-}C_5Me_5)(C_3S_5)$ (120 mg, 0.30 mmol), a dichloromethane (5 cm^3) solution of bromine (0.38 cm^3, 0.15 mmol) was added with stirring resulting in the dark green solution turning dark violet. To the solution, hexane (200 cm^3) was added by stirring for 5 min to afford fine, dark violet needles of **4**, which were collected by filtration, washed with hexane, and dried in vacuo (60% yield). Anal. found: C, 32.52; H, 3.48%. $C_{13}H_{15}BrCoS_5$ requires C, 33.19; H, 3.21%. To the above dichloromethane solution saturated with **4**, an equi-volume of hexane was slowly added, and the solvents were allowed to stand at 5°C overnight to afford dark violet plates of **4** suitable for the X-ray structural analysis.

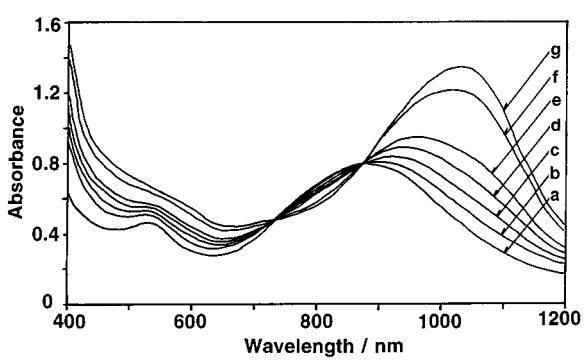

Fig. 3. Electronic absorption spectra of **1** (2.5×10^{-4} mol dm^{-3}) in dichloromethane in the presence of iodine. Concentration of iodine: (a) 0; (b) 1.2×10^{-4}; (c) 1.8×10^{-4}; (d) 2.4×10^{-4}; (e) 3.0×10^{-4}; (f) 6.0×10^{-4}; (g) 7.5×10^{-4} mol dm^{-3}.

2.6. Physical measurements

Electronic absorption, IR, ESR [22] and powder reflectance spectra [23] were recorded as described previously. ^{1}H-NMR spectra were recorded at 270 MHz, using a JEOL EX-270 spectrometer, the chemical shifts being measured relative to tetramethylsilane as an internal standard in C_6D_6. Raman spectra were measured using a JASCO R-800 spectrophotometer at the Graduate School of Science, Osaka University. X-ray photoelectron spectra were obtained by irradiating the complexes with Mg–K_α X-rays (300 W) at 298 K using an ULVAC-PHI ESCA 5700 photoelectron spectrometer at Osaka Municipal Technical Research Institute, and were calibrated with the carbon $1s_{1/2}$ photoelectron peak (285 eV). An electrospray ionization (ESI) mass spectrum was obtained as described previously [24]. A cyclic voltammogram of complex **1** in *N*,*N*-dimethylformamide was measured using [N^nBu_4][ClO_4] as an electrolyte, as described previously [25]. Electrical resistivities of the complexes were measured at r.t. for compacted pellets by the conventional two-probe method [26].

2.7. MO calculations

The density functional theory (DFT) calculation was performed with the hybrid functional B3PW91 method [27,28] using the Gaussian 94 program suite [29] on an SX-4R/64M2 computer (NEC Co.) at the Computation Center of Osaka University. The effective core potential approximation was also incorporated into the DFT calculation via the use of the built-in LanL2DZ basis function set [30].

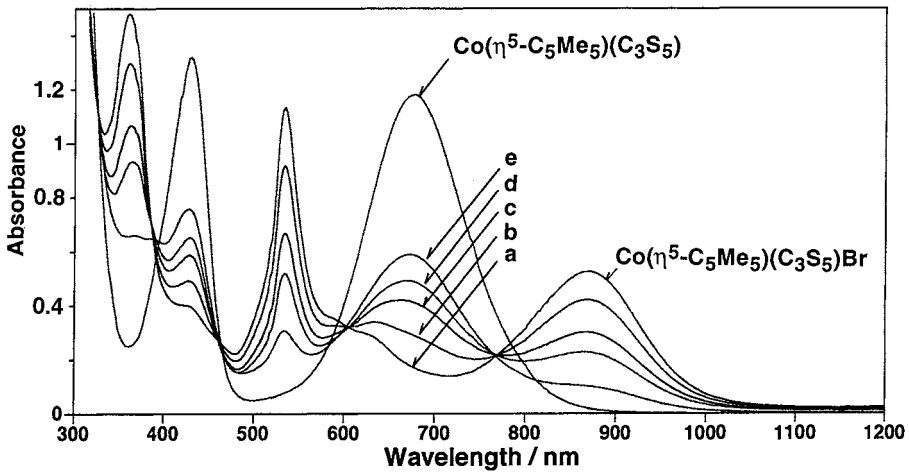

Fig. 5. Time-dependent spectral change of $Co(\eta^5\text{-}C_5Me_5)(C_3S_5)$ (1.0×10^{-4} mol dm^{-3}) by addition of an equimolar amount of bromine in dichloromethane. Time: (a) 0; (b) 100; (c) 400; (d) 760; (e) 3000 s.

2.8. Crystal structure determination of complex **4**

Diffraction data were collected on a Rigaku AFC-7R four-circle diffractometer with a graphite-monochromated Mo–K_α ($\lambda = 0.71069$ Å) radiation at the Graduate School of Science, Osaka University. Crystallographic data are summarized in Table 1.

The unit-cell parameters were determined from 25 independent reflections with 2θ over the range of 24.0°–24.8°. Three standard reflections were monitored after every 150 reflections. No significant decays in their intensities were observed throughout the data collection. The reflection data were corrected for Lorentz and polarization effects, together with absorption [31] (transmission factors, 0.593–1.000).

The structure was solved by the direct method (SHELXS86) [32] and refined on F by the full-matrix least-squares technique. All the non-hydrogen atoms were refined anisotropically and the hydrogen atoms isotropically. Calculations were performed with the TEXSAN structure analysis package [33] on an IRIS INDIGO workstation at the Graduate School of Science, Osaka University. Atomic scattering factors were taken from the usual sources [34]. Final atomic co-ordinates are given in Table 2. Figs. 8 and 9 were drawn with a local version of ORTEP II [35].

3. Results and discussion

3.1. Properties of complex **1** and its oxidized species **2** and **3**

Fig. 1 shows the positive ion ESI mass spectrum of **1** dissolved in dichloromethane. The peak at m/z 479.4 ($z = +1$) is due to the $[Co(\eta^5\text{-}C_5H_5)(C_8H_4S_8)]^+$ cation. The calculated mass spectrum on the isotope distribution of the cation species is in good agreement with the observed spectrum having the interval of 1.0 (the enlarged spectrum). $Co(\eta^5\text{-}C_5H_5)(C_8H_4S_8)$ has a rather

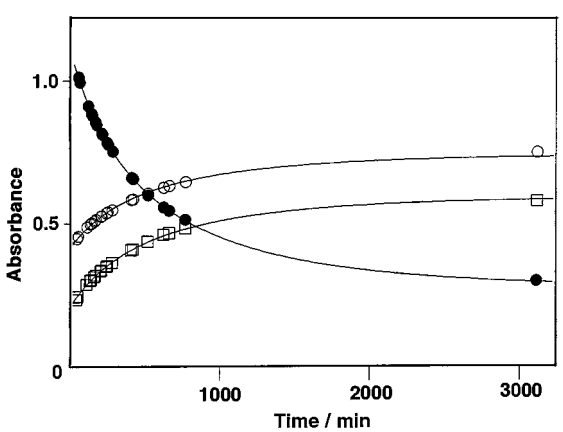

Fig. 6. Time-dependency of absorbances at 428 (○), 676 (□) and 534 nm (●) in the reaction of $Co(\eta^5\text{-}C_5Me_5)(C_3S_5)$ (1.0×10^{-4} mol dm^{-3}) with 0.5 molar amounts of bromine in dichloromethane. Lines are calculated by Eq. (2) for the above reaction.

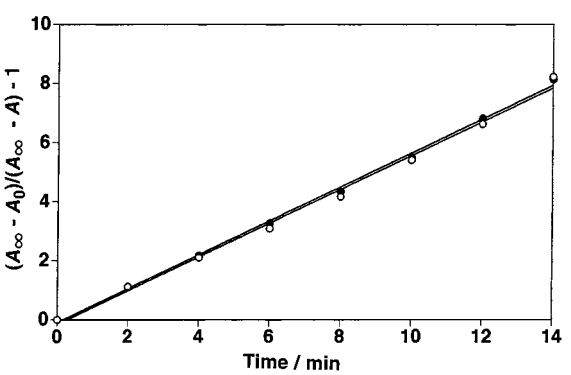

Fig. 7. Time-dependency of absorbances at 528 (○) and 676 nm (●) in the reaction of $Co(\eta^5\text{-}C_5H_5)(C_3S_5)$ (1.0×10^{-4} mol dm^{-3}) with 0.5 molar amounts of bromine in dichloromethane. Lines are calculated by Eq. (3) for the above reaction.

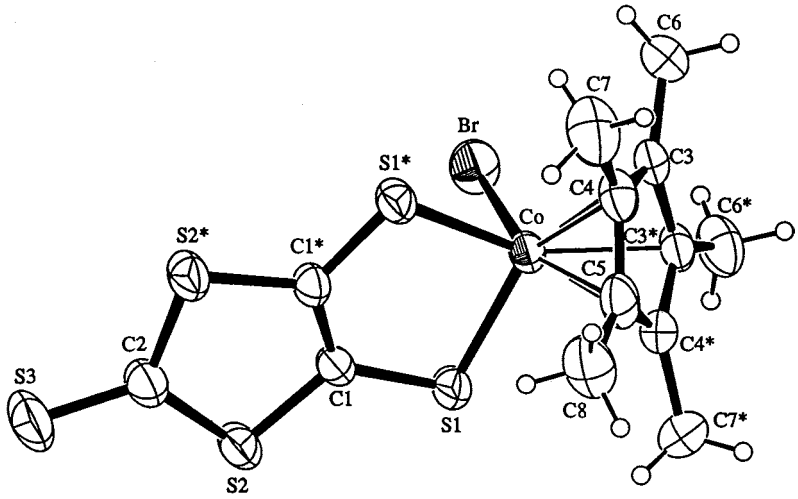

Fig. 8. Molecular geometry of **4** together with the atomic numbering scheme. Thermal ellipsoids are shown at the 50% probability level. Atoms are related to starred ones by a mirror symmetry.

low oxidation potential, as described below, which leads to the oxidation of the complex through the electrolysis at the electrospray inlet.

A cyclic voltammogram of **1** in *N*,*N*-dimethylformamide is shown in Fig. 2. It exhibits reversible redox potentials at -0.63 and $+0.45$ V (versus SCE) for $[Co(\eta^5C_5H_5)(C_8H_4S_8)]^-/[Co(\eta^5\text{-}C_5H_5)(C_8H_4S_8)]^0$ and $[Co(\eta^5\text{-}C_5H_5)(C_8H_4S_8)]^0/[Co(\eta^5\text{-}C_5H_5)(C_8H_4S_8)]^+$ processes, respectively. The rather low redox potentials are in contrast to those of the corresponding C_3S_5 complex (-0.544 and $+0.638$ V versus SCE in acetonitrile) [10]. Oxidation potentials of other $C_8H_4S_8$–metal complexes ($[N^nBu_4][Au(C_8H_4S_8)_2]$ [4] and $[N^nBu_4]_2[Pt(C_8H_4S_8)_2]$ [5,6]) were also observed to be lower than those of the corresponding C_3S_5–metal complexes.

Fig. 3 shows the spectral change of **1** on adding various amounts of iodine as an oxidant. Addition of excess amounts of the oxidant gives the final spectrum of the $[Co(\eta^5\text{-}C_5H_5)(C_8H_4S_8)]^+$ species. The band at 880 nm due to the intramolecular charge transfer (CT) transition from the cyclopentadienyl group to the Co(III) ion/$C_8H_4S_8$ ligand moiety is shifted to 1040 nm with isosbestic points upon the oxidation. Similar spectral changes are observed for the one-electron oxidation of $Co(\eta^5\text{-}C_5H_5)(C_3S_5)$ and $Co(\eta^5\text{-}C_5Me_5)(C_3S_5)$, as described below.

A reaction of **1** with an excess amount of iodine has afforded complex **2** as an oxidized species. The Raman spectrum of **2** has exhibited a scattering band at 111 cm^{-1}, which is assigned to the symmetric stretching of the I_3^- ion [36,37]. This indicates that **2** is a one-electron oxidized species. In accordance with this, **2** has exhibited an intense sharp ESR signal at $g = 2.01$ (peak-to-peak linewidth, 2.5 mT). The signal observed at $g = 2.01$ is ascribed to the radical species of the $C_8H_4S_8$ ligand moiety, as observed for the radicals of sulfur-rich compounds; the tetrathiafulvalenium radical cation [38,39] and partially oxidized $C_8H_4S_8$–metal (Pt(II) [6] and Mo(IV) [40]) and C_3S_5–metal (Cu(I), Au(III), Re(IV), Mo(IV) and W(IV)) complexes [21,23,39,41] with the ligand-centered oxidation. Thus, in complex **2** the $C_8H_4S_8$ ligand-centered oxidation is also likely to occur. Upon the ligand-centered oxidation, the C=C stretching IR bands of the $C_8H_4S_8$ ligand have appeared at lower frequencies (1397 and 1218 cm^{-1}) compared with those of the unoxidized species **1** (1446 and 1258 cm^{-1}), as observed for some C_3S_5–metal (Fe(II), Ni(II) and Au(III)) complexes [25,39,42]. This is consistent with the fact that the binding energies of the cobalt $2p_{1/2}$ and $2p_{3/2}$ electrons for the oxidized species **2** determined by XPS are 794.9 and 780.0 eV, respectively, which are essentially the same as those (795.1 and 779.9 eV) for the unoxidized species **1**. Complex **3** is formally a 0.7-electron oxidized species. It has shown a broad C=C stretching IR band at 1215 cm^{-1}, which is lower by 43 cm^{-1} than that of **1**. The ESR signal has appeared at $g = 2.01$ (peak-to-peak linewidth, 1.1 mT). These findings support the $C_8H_4S_8$ ligand-centered oxidation for this oxidized species.

The oxidized species **2** and **3** have exhibited electrical conductivities of 0.19 and 0.16 S cm^{-1}, respectively, measured for compacted pellets at r.t., although the unoxidized complex **1** is essentially an insulator (the electrical conductivity, $< 10^{-8}$ S cm^{-1}). The high conductivities come from an effective molecular packing favorable for the electron-conduction. At first sight, the molecules seem to be inadequate for the packing in the solid state because the η^5-C_5H_5 ring is considered to be perpendicular to the $Co(C_8H_4S_8)$ moiety. However, the extended π-system having many sulfur atoms in this ligand may form a molecular interaction array through several S–S non-bonded contacts in the solid state, as depicted in Fig. 4. The powder reflectance spectrum of **2** has shown an appreciable band at 1400 nm besides

Table 3
Selected bond distances (Å) and angles (°) for **4**

Co–Br	2.3951(9)	Co–S(1)	2.2173(9)	Co–C(3)	2.106(3)
Co–C(4)	2.093(3)	Co–C(5)	2.053(5)	S(1)–C(1)	1.693(3)
S(2)–C(1)	1.741(3)	S(2)–C(2)	1.737(3)	S(3)–C(2)	1.628(5)
C(1)–C(1*)	1.384(6)	C(3)–C(3*)	1.438(6)	C(3)–C(4)	1.419(4)
C(3)–C(6)	1.487(5)	C(4)–C(5)	1.427(4)	C(4)–C(7)	1.495(6)
C(5)–C(8)	1.509(8)				
Br–Co–S(1)	91.92(3)	Br–Co–C(3)	92.86(9)		
Br–Co–C(4)	126.1(1)	Br–Co–C(5)	158.8(2)		
S(1)–Co–S(1*)	91.50(5)	S(1)–Co–C(3)	153.77(9)		
S(1)–Co–C(3*)	114.08(9)	S(1)–Co–C(4)	141.8(1)		
S(1)–Co–C(4*)	89.84(9)	S(1)–Co–C(5)	102.7(1)		

the bands of the complex molecule itself. This band is likely ascribed to the molecular interaction. Even complex **4**, having the C_3S_5 ligand, has a one-dimensional interaction by some S–S contacts in the solid state, as described below. Oxidized, non-planar oxomolybdenum complexes, $[Mo(O)(C_8H_4S_8)_2]^{n-}$ $(n<1)$ species, also have recently been found to exhibit high electrical conductivities [40]. Thus, these findings suggest that the $C_8H_4S_8$ ligand is very effective for the construction of the electron-conduction pathway of the metal complexes in the solid state.

3.2. Oxidation of $Co(\eta^5\text{-}C_5H_5)(C_3S_5)$ and $Co(\eta^5\text{-}C_5Me_5)(C_3S_5)$

Since the first oxidation potentials of these complexes ($E_{1/2}=0.388$ and 0.211 V, respectively, versus Ag/Ag^+ in acetonitrile [10]) are somewhat high, they have not been oxidized by iodine. However, bromine has oxidized these complexes to afford the one-electron oxidized species in solution.

$Co(\eta^5\text{-}C_5Me_5)(C_3S_5)Br$ (**4**) has been isolated as crystals and the structure has been determined by X-ray crystallography, as described below. This oxidized Co(III) species has the Co–Br bond in the solid state. It has exhibited the isotropic ESR spectrum ($g=2.016$) in dichloromethane, which consists of an octet (^{59}Co, $I=7/2$) of quartets ($^{79}Br(50.54\%)$ and $^{81}Br(49.46\%)$, $I=3/2$); ^{59}Co and $^{79/81}Br$ hyperfine couplings are 1.9 and 2.8×10^{-3} cm^{-1}, respectively [19]. This finding also confirms the Co–Br bond in solution. These small values indicate insubstantial spin densities on Co and Br atoms and most of them on the C_3S_5 ligand. Mulliken spin densities for **4** evaluated by a DFT calculation [27–29] have shown the presence of 90% spins on the C_3S_5 ligand (75% spins on the sulfur atoms); Co, 0.005; Br, 0.058; S(1), S(1*), 0.322; S(2), S(2*); −0.01; S(3), 0.121; C(1), C(1*), 0.084; C(2), −0.016; C(3)–C(8) (the C_5Me_5 ring), −0.011– +0.045 (atomic numbering scheme, see Fig. 8) [19]. In the solid ESR spectrum of **4** a broad signal has been observed at $g=2.01$ (peak-to-peak linewidth, 10.7 mT). These findings suggest the C_3S_5 ligand-centered oxidation, which was observed for some C_3S_5–metal complexes [21–24,39,41]. In accordance with these findings, the Co–S distances of **4** are somewhat longer than those of $Co(\eta^5\text{-}C_5Me_5)(C_3S_5)$, as described below, and the C=C stretching IR frequency (1350 cm^{-1}) of **4** is somewhat lower than that (1394 cm^{-1}) of $Co(\eta^5\text{-}C_5Me_5)(C_3S_5)$. Furthermore, the binding energies (794.9 and 779.9 eV) of Co $2p_{1/2}$ and $2p_{3/2}$ electrons of **4** determined by XPS are very close to those (795.4 and 780.3 eV) of $Co(\eta^5\text{-}C_5Me_5)(C_3S_5)$ [19].

In the solid state, the oxidized species **4** has molecular interaction through S–S non-bonded contacts, as shown below, and it exhibits a strong antiferromagnetic interaction [19]. However, it has very low electrical conductivity; 7.9×10^{-8} S cm^{-1} measured for a compacted pellet at r.t. Although the complex is in the oxidized state to enhance the S–S contacts, the molecular interaction seems to be insufficient for the electron-conduction.

A dichloromethane solution containing $Co(\eta^5\text{-}C_5H_5)(C_3S_5)$ and 0.5 molar amount of bromine has also exhibited an isotropic ESR signal consisting of an octet of quartets at $g=2.008$, which is very close to that of **4** in dichloromethane. This finding indicates the formation of $Co(\eta^5\text{-}C_5H_5)(C_3S_5)Br$. However, the signal has quickly decreased in its intensity within 30 min. This indicates that the paramagnetic species is unstable, followed by the fast disproportionation to $Co(\eta^5\text{-}C_5H_5)(C_3S_5)$ and the two-electron oxidized species, as described below.

The time-dependent spectral change of $Co(\eta^5\text{-}C_5Me_5)(C_3S_5)$ in dichloromethane by addition of an equimolar amount of bromine at r.t. is shown in Fig. 5. $Co(\eta^5\text{-}C_5Me_5)(C_3S_5)$ exhibits intense bands at 428 and 676 nm, which are ascribed to the π–π^* transition of the C_3S_5 ligand and an intramolecular CT transition from the C_5Me_5 group to the Co(III) ion/C_3S_5 ligand, respectively. The addition of bromine to $Co(\eta^5\text{-}C_5Me_5)(C_3S_5)$ has immediately afforded new bands at 534 and 868 nm due to the $Co(\eta^5\text{-}C_5Me_5)(C_3S_5)Br$, accompanied with the decrease of the band at 676 nm

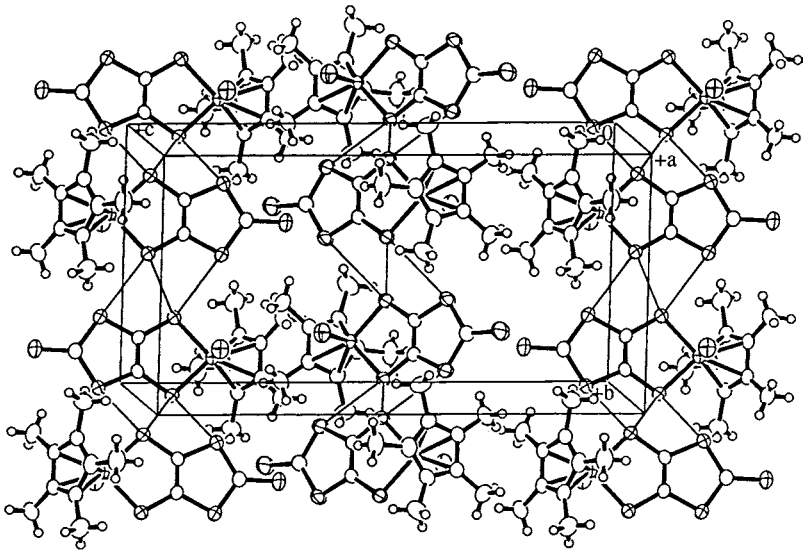

Fig. 9. Packing diagram of **4**. Fine lines represent S···S non-bonded contacts less than 3.8 Å.

due to the unoxidized species, Co(η^5-C_5Me_5)(C_3S_5). After the formation of this one-electron oxidized species, the intensities of the bands at 534 and 868 nm have decreased with time, concomitantly accompanied with the increase of the band intensity at 676 nm. Thus, assuming the disproportionation reaction of the one-electron oxidized complex to the unoxidized species and the further oxidized one (Eq. (1)), the reaction process has been analyzed. Absorbances at three absorption maxima are plotted against time (Fig. 6). They can be fitted by the calculated curves according to Eq. (2).

$$2[\mathrm{Co}(\eta^5\text{-}\mathrm{C_5Me_5})(\mathrm{C_3S_5})\mathrm{Br}] \underset{k_{con}}{\overset{k_{dis}}{\rightleftharpoons}} [\mathrm{Co}(\eta^5\text{-}\mathrm{C_5Me_5})(\mathrm{C_3S_5})] + [\mathrm{Co}(\eta^5\text{-}\mathrm{C_5Me_5})(\mathrm{C_3S_5})\mathrm{Br_2}] \quad (1)$$

$$A = A_0(A_\infty - A_0)\frac{(ck_{dis} + k)\sinh(kt)}{ck_{dis}\sinh(kt) + k\cosh(kt)} \quad (2)$$

A is an observed absorbance, A_0 the initial absorbance of Co(η^5-C_5Me_5)(C_3S_5)Br, A_∞ the final absorbance, and t a time after the addition of bromine. $A = ck_{dis}/2$, $B = ck_{con}/2$ and $k = (c/2)(k_{dis}k_{con})^{1/2}$, where c is a concentration of Co(η^5-C_5Me_5)(C_3S_5) before the addition of bromine. The fitting curves are in agreement with the observed absorbances, indicating the reasonable disproportionation reaction. The reaction rates are determined: $k_{dis} = 17$ and $k_{con} = 5.0$ mol dm^{-3} min^{-1}. In the final equilibrium, the amounts of the species are estimated: Co(η^5-C_5Me_5)(C_3S_5)Br (20%), Co(η^5-C_5Me_5)(C_3S_5) (40%), and Co(η^5-C_5Me_5)(C_3S_5)Br_2 (40%). From the spectrum in the final state, the two-electron oxidized species is deduced to have absorption bands at 380 and 620 nm.

The absorption spectrum of Co(η^5-C_5H_5)(C_3S_5) in dichloromethane has exhibited bands at 430 and 676 nm, which are similar to those of Co(η^5-C_5Me_5)(C_3S_5). The reaction of Co(η^5-C_5H_5)(C_3S_5) with bromine in dichloromethane has given Co(η^5-C_5H_5)(C_3S_5)Br, showing the bands at 360, 528 and 800 nm. This oxidized species also has been rapidly disproportionated to the unoxidized complex and the two-electron oxidized one, of which the latter species has further decomposed finally to give insoluble yellow solids of C_6S_8 [10]. Considering only the forward process (k_{dis}) of the disproportionation reaction of the one-electron oxidized complex, Eq. (3) is derived,

$$\frac{A_\infty - A_0}{A_\infty - A} - 1 = ck_{dis}t \quad (3)$$

where c is a concentration of Co(η^5-C_5H_5)(C_3S_5)Br and A, A_0, and A_∞ are absorbances at an arbitrary time, initial and final stages, respectively. Plots of $[(A_\infty - A_0)/(A_\infty - A)] - 1$ versus time (t) for these bands at 528 and 676 nm show a linear relationship (Fig. 7). This finding indicates a second-order reaction for the disproportionation of the Co(η^5-C_5H_5)(C_3S_5)Br in solution. k_{dis} is calculated to be 5.71×10^3 mol dm^{-3} min^{-1}, which is very large compared with that of Co(η^5-C_5Me_5)(C_3S_5)Br.

3.3. Crystal structure of complex *4*

Fig. 8 shows the molecular structure of **4**, together with atomic numbering scheme. Bond distances and angles are listed in Table 3. The molecule has a mirror containing Co, Br, C(2), C(5), C(8) and S(3) atoms. The Co(C_3S_5) unit is almost planar (± 0.05 Å) and makes an angle of 58.7° with the C_5Me_5 ring plane. This is in contrast to that (87.8°) of Co(η^5-C_5Me_5)(C_3S_5) [18], which is caused by the ligation of the Br atom in **4**. The Co–Br bond (2.3951(9) Å) agrees well with those

(2.338–2.49 Å) found in octahedral Co(III) complexes [43–46]. The Co–S(1) distance (2.2173(9) Å) is longer than the Co–S distances (2.135(2) and 2.138(2) Å) of Co(η^5-C_5Me_5)(C_3S_5) [18]. This is due to the somewhat decreased co-ordination ability of the C_3S_5 ligand upon the C_3S_5 ligand-centered oxidation.

In the C_3S_5 moiety, the S(1)–C(1) bond (1.693(3) Å) is appreciably short compared with S(2)–C(1) (1.741(3) Å) and S(2)–C(2) bonds (1.737(1) Å). This feature in the C_3S_5 ligand was also observed for Co(η^5-C_5H_5)(C_3S_5), Co($\eta^5C_5Me_5$)(C_3S_5) [18], and the oxidized C_3S_5–nickel complexes, Ni(η^5-C_5H_5)(C_3S_5) [17], Ni(C_3S_5)$_2$ [47], [guanidium][Ni(C_3S_5)$_2$]$_2$ [48] and [PPh_4][Ni(C_3S_5)$_2$]$_3$ [49], which is in contrast to the cases of [N^{n}Bu$_4$]$_2$[Ni(C_3S_5)$_2$] [50], [N^{n}Bu$_4$][Au(C_3S_5)$_2$] [39], and [Et-NC_5H_5]$_2$[Cu(C_3S_5)$_2$] [51] without appreciable differences among the C–S bond distances. The Co–C distances (2.053(5)–2.106(3) Å) are comparable with those (average, 2.057(7) Å) of Co(η^5-C_5Me_5)(C_3S_5) [18] and those (2.03–2.08 Å) found for several cobaltocenium salts [52–56].

The crystal structure reveals a one-dimensional array of the molecules through two short non-bonded S–S contacts (S(1)–S(2)($2-x$, $-y$, $-z$), 3.667(1) and S(1)–S(1)($2-x$, $-y$, $-z$), 3.791(2) Å) along the *b*-axis, as illustrated in Fig. 9. Such S–S interactions were not observed for Co(η^5-C_5Me_5)(C_3S_5) (the nearest S–S contact, 3.869(5) Å) [18]. The C_3S_5 ligand-centered oxidation in **4** seems to enhance intermolecular S–S non-bonded contacts in the solid state.

4. Supplementary material

Tables of all hydrogen atomic co-ordinates, tables of anisotropic thermal parameters, lists of bond lengths and angles, and structure factors are available from the authors on request.

Acknowledgements

The authors acknowledge Professors S. Suzuki, T. Ohno (Graduate School of Science, Osaka University) and R. Arakawa (Kansai University) for the measurements of ESR, Raman and electrospray ionization mass spectra, respectively, and Dr I. Kawafune (Osaka Municipal Technical Research Institute) for the measurement of X-ray photoelectron spectra. This research was supported in part by a Grant-in-Aids for Scientific Research No. 09540665 and a Grant-in-Aids on Priority Areas No. 09239231 from Ministry of Education, Science, Sports and Culture, Japan.

References

[1] P. Cassoux, L. Valade, K. Kobayashi, A. Kobayashi, R.A. Clark, A.E. Underhill, Coord. Chem. Rev. 110 (1991) 115.
[2] G. Matsubayashi, Reviews on Heteroatom Chemistry, vol. 4, Myu, Tokyo, 1991, p. 171.
[3] R.-M. Olk, B. Olk, W. Dietzsch, R. Kirmse, E. Hoyer, Coord. Chem. Rev. 117 (1992) 99.
[4] M. Nakano, A. Kuroda, T. Maikawa, G. Matsubayashi, Mol. Cryst. Liq. Cryst. 284 (1996) 301.
[5] M. Nakano, A. Kuroda, G. Matsubayashi, Inorg. Chim. Acta 254 (1997) 189.
[6] M. Nakano, A. Kuroda, H. Tamura, R. Arakawa, G. Matsubayashi, Inorg. Chim. Acta 279 (1998) 165.
[7] N.L. Narvor, N. Robertson, E. Wallace, J.D. Kilburn, A.E. Underhill, P.N. Bartlett, M. Webster, J. Chem. Soc. Dalton Trans. (1996) 823.
[8] N.L. Narvor, N. Robertson, T. Weyland, J. D. Kilburn, A.E. Underhill, M. Webster, N. Svenstrup, J. Becher, J. Chem. Soc. Chem. Commun. (1996) 1363.
[9] X. Yang, T.B. Rauchfuss, S.R. Wilson, J. Am. Chem. Soc. 111 (1989) 3465.
[10] H. Ushijima, S. Sudoh, M. Kajitani, K. Shimizu, T. Akiyama, A. Sugimori, Inorg. Chim. Acta 175 (1990) 11.
[11] H. Ushijima, S. Sudoh, M. Kajitani, K. Shimizu, T. Akiyama, A. Sugimori, Appl. Organomet. Chem. 5 (1991) 221.
[12] F. Guyon, C. Lenoir, M. Fourmigue, J. Larsen, J. Amaudrut, Bull. Soc. Chim. Fr. 131 (1994) 217.
[13] F. Guyon, J. Amaudrut, M.-F. Mercier, K. Shimizu, J. Organomet. Chem. 465 (1994) 187.
[14] F. Guyon, M. Foumigue, P. Audebert, J. Amaudrut, Inorg. Chim. Acta 239 (1995) 117.
[15] M. Fourmigue, C. Lonoir, C. Coulon, F. Guyon, J. Amaudrut, Inorg. Chem. 34 (1995) 4979.
[16] S. Inomata, H. Takano, K. Hiyama, H. Tobita, H. Ogino, Organometallics 14 (1995) 2112.
[17] C. Faulmann, F. Delpech, I. Malfant, P. Cassoux, J. Chem. Soc. Dalton Trans. (1996) 2261.
[18] M. Fourmigue, V. Perrocheau, Acta Crystallogr. C53 (1997) 1213.
[19] H. Mori, M. Nakano, H. Tamura, G. Matsubayashi, W. Mori, Chem. Lett. (1998) 729.
[20] R.F. Heck, Inorg. Chem. 4 (1965) 855.
[21] K. Akiba, G. Matsubayashi, T. Tanaka, Inorg. Chim. Acta 165 (1989) 245.
[22] G. Matsubayashi, K. Douki, H. Tamura, M. Nakano, Inorg. Chem. 32 (1993) 5990.
[23] G. Matsubayashi, S. Tanaka, A. Yokozawa, J. Chem. Soc. Dalton Trans. (1992) 1827.
[24] G. Matsubayashi, T. Maikawa, H. Tamura, M. Nakano, R. Arakawa, J. Chem. Soc. Dalton Trans. (1996) 1539.
[25] S. Tanaka, G. Matsubayashi, J. Chem. Soc. Dalton Trans. (1992) 2837.
[26] K. Ueyama, G. Matsubayashi, T. Tanaka, Inorg. Chim. Acta 87 (1984) 143.
[27] A.D. Becke, J. Chem. Phys. 98 (1993) 5648.
[28] J.P. Perdew, Y. Wang, Phys. Rev. B 45 (1992) 13244.
[29] Gaussian 94, Revision D.4, M.J. Frisch, G.W. Trucks, H.B. Schlegel, B.G. Johnson, M.A. Lobb, J.R. Cheeseman, P.M.W. Keith, G.A. Petersson, J.A. Montgomery, K. Raghavachari, M.A. Al-Laham, V.G. Zakrzewski, J.V. Ortiz, J. B. Foresman, J. Cioslowski, B.B. Stevanov, A. Nanayakkara, M. Challacombe, C.Y. Peng, P.Y. Ayala, W. Chen, M.W. Wong, J.L. Andres, E.S. Replogle, R. Gomperts, R.L. Martin, D.J. Fox, J.S. Binkley, D.J. Defrees, J. Baker, J.P. Stewart, M. Head-Gordon, C. Gonzalez, J.A. Pople, Gaussian Inc., Pittsburgh, PA, 1995.

[30] P.J. Hay, W.R. Wadt, J. Chem. Phys. 82 (1985) 270.
[31] A.C.T. North, D.C. Philips, F.C. Mathews, Acta Crystallogr. Sect. A 24 (1968) 351.
[32] G.M. Sheldrick, SHELXS86, a computer program for the solution of crystal structures, University of Göttingen, Germany, 1985.
[33] TEXSAN, a crystal structure analysis package, Molecular Structure Corp., The Woodlands, TX, 1992.
[34] International Tables for X-Ray Crystallography, vol. 4, Kynoch, Birmingham, UK, 1974.
[35] C.K. Johnson, ORTEP-II, Rep. ORNL-5138, Oak Ridge National Laboratory, Oak Ridge, TN, 1976.
[36] T.J. Marks, D.W. Kalina, in: J.S. Miller (Ed.), Extended Linear Chain Compounds, vol. 1, Plenum Press, New York, 1982, p. 197.
[37] B.N. Diel, T. Inabe, J.W. Lyding, K.F. Schoch Jr., C.R. Kannewurf, T.J. Marks, J. Am. Chem. Soc. 105 (1983) 1551.
[38] G. Matsubayashi, K. Yokoyama, T. Tanaka, J. Chem. Soc. Dalton Trans. (1988) 253.
[39] G. Matsubayashi, A. Yokozawa, J. Chem. Soc. Dalton Trans. (1990) 3535.
[40] G. Matsubayashi, T. Yonamine, M. Nakano, to be published.
[41] A. Yokozawa, G. Matsubayashi, Inorg. Chim. Acta 186 (1991) 165.
[42] Y. Sakamoto, G. Matsubayashi, T. Tanaka, Inorg. Chim. Acta 113 (1986) 137.
[43] B.F. Hoskins, R. Robson, G.A. Williams, Inorg. Chim. Acta 16 (1976) 121.
[44] G. Bombieri, E. Forsellini, A. Del Pia, M. L. Tobe, C. Chatterjee, Inorg. Chim. Acta 68 (1983) 205.
[45] M. Megnamisi-Belombe, Acta Crystallogr. C39 (1983) 705.
[46] C. Lopez, S. Alvarez, X. Solans, M. Font-Attaba, Inorg. Chem. 25 (1986) 2962.
[47] L. Valade, J.-P. Legros, M. Bousseau, P. Cassoux, M. Garbauskas, M. Interrante, J. Chem. Soc. Dalton Trans. (1985) 783.
[48] O. Lindqvist, L. Sjolin, J. Sieler, G. Steimecke, E. Hoyer, Acta Chem. Scand. Ser. A 33 (1979) 445.
[49] Y.S.J. Veldhuizen, N. Veldman, A.L. Spek, C. Faulmann, J.G. Haasnoot, J. Reedijk, Inorg. Chem. 34 (1995) 140.
[50] T. Nakamura, A.E. Underhill, A.T. Coomber, R.H. Friend, H. Tajima, A. Kobayashi, H. Kobayashi, Inorg. Chem. 34 (1995) 870.
[51] G. Matsubayashi, K. Takahashi, T. Tanaka, J. Chem. Soc. Dalton Trans. (1988) 967.
[52] E. Frasson, G. Bombieria, C. Parattoni, Acta Crystallogr. Sect. A 16 (1963) 68.
[53] M.R. Churchill, J.P. Fonnessey, Inorg. Chem. 7 (1968) 1123.
[54] M.R. Churchill, B.G. DeBoer, J. Am. Chem. Soc. 96 (1974) 6310.
[55] P.E. Riley, E.E. Davis, J. Organomet. Chem. 152 (1978) 209.
[56] Q. Fang, X.-Z. You, J.-H. Cai, M.-Y. He, Acta Crystallogr. Sect. C 49 (1993) 1347.